

## Supporting Information

### **Tailoring Phase Alignment and Interfaces via Polyelectrolyte Anchoring Enables Large-Area 2D Perovskite Solar Cells**

*C. Han, Y. Wang, J. Yuan, J. Sun, X. Zhang, C. Cazorla, X. Wu, Z. Wu, J. Shi, J. Guo, H. Huang, L. Hu, X. Liu, H. Y. Woo, J. Yuan\*, W. Ma*

## 1. Materials

Butylamine hydroiodide (BAI, 99.5%), Methylammonium iodide (MAI, 99.5%), Poly(3,4-ethylenedioxythiophene):poly(styrenesulfonate) (PEDOT:PSS), Bathocuproine (BCP, 99%) and Poly[bis(4-phenyl)(2,4,6-trimethylphenyl)amine] (PTAA) were purchased from Xi'an Polymer Light Technology Corp.. Lead (II) iodide ( $\text{PbI}_2$ , 99.999%) and Potassium hydroxide (KOH, 99.98%) were both purchased from Alfa Aesar. (6,6)-Phenyl-C61-butyric acid methyl ester ( $\text{PC}_{61}\text{BM}$ , 99%), Poly[3-(4-carboxybutyl) thiophene-2,5-diy] (P3CT) were purchased from 1-Materials. N,N-dimethylformamide (DMF, 99.8%), Dimethyl sulfoxide (DMSO, 99.8%), Chlorobenzene (CB, 99.8%), Isopropanol (IPA, 99.8%) and Butylamine (BA, 99.8%) were all purchased from Sigma-Aldrich. Unless otherwise stated, all of the chemicals were obtained commercially and used directly without purification.

## 2. Solution preparation

P3CT-K/P3CT-BA colloidal solution was prepared by dissolving P3CT with KOH/BA (weight ratio 4:5.7/4:7.3, excess KOH/BA) in deionized water ( $10 \text{ mg mL}^{-1}$ ) and stirred at  $60 \text{ }^\circ\text{C}$  for 72 h. Before using, dilute the solution to  $0.5 \text{ mg mL}^{-1}$ ,  $1.0 \text{ mg mL}^{-1}$ ,  $1.5 \text{ mg mL}^{-1}$ ,  $2.0 \text{ mg mL}^{-1}$ ,  $2.5 \text{ mg mL}^{-1}$ ,  $3.0 \text{ mg mL}^{-1}$ ,  $4.0 \text{ mg mL}^{-1}$  with deionized water and filter with aqueous filter. To prepare the  $\text{BA}_2\text{MA}_3\text{Pb}_4\text{I}_{13}$  perovskite precursor, the mixed powder containing BAI (0.45 M), MAI (0.675 M), and  $\text{PbI}_2$  (0.9 M) were added into mixed solvent of DMF and DMSO (97:3 v/v), and stirring at room temperature overnight. Precursor solution of ETL was prepared by dissolving 20 mg  $\text{PC}_{61}\text{BM}$  into 1 mL chlorobenzene. The concentration of BCP was 1 mg/ml in isopropanol.

## 3. Device fabrication

The patterned ITO substrates were cleaned by sonication in deionized water, isopropyl alcohol, and acetone sequentially and then dried with nitrogen and store in a drying cabinet before use. The cleaned ITO glass substrates were treated using an ultraviolet zone for 15 min. The hole transporting layer was attained by spin-coating the P3CT-X solution onto the treated ITO with a speed of 3000 rpm for 40 s, and then thermally annealing at 140 °C for 15 minutes. The BA<sub>2</sub>MA<sub>3</sub>Pb<sub>4</sub>I<sub>13</sub> active layer was prepared on to the ITO/P3CT-X substrates in N<sub>2</sub> atmosphere with a hot-cast process. The substrates containing P3CT-K/P3CT-BA were preheated at 75 °C for 5 min, and then transferred onto the sucker of a spin coater. Right after that, 30 μL of perovskite precursor solutions were applied and spun coated at 4500 rpm for 20 s. The resulting BA<sub>2</sub>MA<sub>3</sub>Pb<sub>4</sub>I<sub>13</sub> films were thermally annealed at 100 °C for 10 min in N<sub>2</sub> glove box. Subsequently, PC<sub>61</sub>BM and BCP were deposited on top of the perovskite layer in turn by spin coating respectively at 2000 rpm for 30 s and 2500 rpm for 30 s. Finally, 80 nm of Ag cathode was evaporated under vacuum  $<2 \times 10^{-6}$  Pa with shadow masks that kept an active area of 0.0725 cm<sup>2</sup>. The device of 1 cm<sup>2</sup> was fabricated by the same spin-coating method as the 0.0725 cm<sup>2</sup> device. A large area of 16 cm<sup>2</sup> of perovskite solar mini-modules, with 7 sub-cells connected in series, was fabricated on the 5×5 cm<sup>2</sup> ITO glass substrates. The series interconnection of the module was constructed by P1, P2, and P3 lines, which were scribed using a laser etching system with the 1064 nm laser. The ITO glass was pre-patterned for P1 by using of laser with 60% output power with a frequency of 80 kHz and pulse width of 10 μs. Then, ITO glass was cleaned by sequentially washing with glass detergent, deionized (DI) water, acetone, and isopropanol (IPA), followed with UV-ozone treatment for 15 min before use. The hole transport layer of P3CT-BA and active layer of 2D perovskite were prepared according to the process described above. C<sub>60</sub> and BCP were deposited by thermal evaporation of 20 nm and 5 nm, respectively. Subsequently, the fabricated

Glass/ITO/P3CT-BA/Perovskite/ETL/BCP layers were scribed by a laser with 15% output power, 65 kHz frequency and 120 ns pulse width for P2 line. Finally, a silver cathode was deposited by thermal evaporation, and Ag layer was scribed for P3 line by a laser with a scribing width of 50  $\mu\text{m}$  with 15% output power, 65 kHz frequency and 120 ns pulse width. The current density-voltage (J-V) characteristics of the devices were performed using a Keithley 2400 digital source meter under simulated AM 1.5G spectrum at 100  $\text{mW cm}^{-2}$  in ambient air conditions with a solar simulator (Class AAA, 94023A-U, Newport). The devices were measured by the forward direction (-0.2 to 1.3 V) and reverse direction (-1.3 to 0.2 V) with a scan rate of 100  $\text{mV s}^{-1}$ . The SPO of devices was measured at a constant bias voltage near the maximum power point and meanwhile recording the continuous current output. The EQE spectra of the cells were characterized through a certified incident photo-to-electron conversion efficiency equipment (Solar Cell Scan 100, Zolix Instruments Co. Ltd.).

#### **4. Characterization**

The UV-vis spectra were recorded on a PerkinElmer model Lambda 750 spectrophotometer. The steady-state and time-resolved PL spectra were measured using a FluoroMax-4 spectrofluorometer (HORIBA Scientific) and Hamamatsu streak camera with a laser of 455 nm, respectively. The UPS spectra were obtained using a Kratos AXIS Ultra DLD ultrahigh vacuum photoemission spectroscopy system, with an Al Ka radiation source. Top-view and cross-section SEM images were characterized by a Zeiss Supra 55 field in high vacuum mode at 15 kV accelerating voltage. AFM images (tapping mode) were captured through an Asylum Research Cypher S AFM microscope. EIS, TPV,  $t$ DOS measurements were carried out through Zahner IM6 electrochemical workstation while applying a bias of under open-circuit with a

frequency between 0.25 MHz and 0.05 Hz under a monochromatic LED (500 nm, 100 mW) light irradiation. GIWAXS patterns of quasi-2D perovskite films were carried out at PLS-II 9A U-SAXS beam line of Pohang Accelerator Laboratory, Korea. X-ray coming from the in-vacuum undulator (IVU) was monochromated ( $E_k = 11.24$  keV,  $\lambda = 1.103$  Å) using a Si (111) double crystal monochromator and focused horizontally and vertically at the sample position (450 (H)×60 (V)  $\mu\text{m}^2$  in FWHM) using K-B-type focusing mirror system. The GIWAXS sample stage was equipped with a 7-axis motorized stage for the fine alignment of the thin sample and the incidence angle of X-rays was adjusted to  $0.12^\circ - 0.14^\circ$ . GIWAXS patterns were recorded with a 2D CCD detector (Rayonix SX165, USA), and X-ray irradiation time was 0.5-5 s depending on the saturation level of the detector. Samples for GIWAXS measurements were prepared by spin-coating polymer solutions on top of the Si substrates.

The transient absorption spectroscopy (TAS) was performed on a Helios pump-probe system (Ultrafast Systems LLC) combined with an amplified femtosecond laser system (Coherent). Optical parametric amplifier (TOPAS-800-fs) provided a 360 nm pump pulse ( $4.2 \mu\text{J}/\text{cm}^2$  at the sample), which was excited by a Coherent Astrella regenerative amplifier (80 fs, 1 kHz, 2.5 mJ per pulse) and seeded with a Coherent Vitara-s oscillator (35 fs, 80 MHz). Samples for TAS measurements were prepared by spin-coating solutions on top of the quartz substrates.

## 5. Density functional theory (DFT)

First-principles calculations based on density functional theory (DFT)<sup>48</sup> were carried out to theoretically analyze the defect properties of  $\text{BA}_2\text{MA}_3\text{Pb}_4\text{I}_{13}$  2D perovskites and the anchoring process of P3CT-BA like molecules on their surface. The generalized gradient approximation (GGA)<sup>49</sup> in the Perdew-Burke-Ernzerhof (PBE) flavor was used to describe the electronic exchange and correlation effects in

the simulated systems. Dispersion interactions between the P3CT-BA like molecules and 2D perovskite surfaces were taken into consideration through the D3 method<sup>50</sup>, and the projector-augmented wave method<sup>51</sup> was employed to represent the ionic cores. The following electronic states were considered as valence: Pb 6*p* and 5*d*; I 4*d* 5*s* and 5*p*; C 2*s* and 2*p*; O 2*s* and 2*p*; H 1*s*; N 2*s* and 2*p*; S 3*s* and 3*p*. A bulk BA<sub>2</sub>MA<sub>3</sub>Pb<sub>4</sub>I<sub>13</sub> perovskite cell containing 204 atoms was first relaxed considering a 2×1×2 Gamma-centered k-point grid and an energy cutoff of 550 eV. Subsequently, a 2x1x2 slab system reproducing the Miller index <001> of the BA<sub>2</sub>MA<sub>3</sub>Pb<sub>4</sub>I<sub>13</sub> perovskite was generated by adding a vacuum region of 30 Å thickness, thus leaving some under-coordinated Pb and I ions and BA and MA molecules at the surface. The simulation supercell contained a total of 816 atoms. A 1×1×1 Gamma-centered k-point grid and an energy cutoff of 400 eV were employed in the slab calculations due to the large computational cost involved. The geometry optimizations were halted when the forces in the atoms were all below 0.005 eV/Å. A third system, involving the <001> BA<sub>2</sub>MA<sub>3</sub>Pb<sub>4</sub>I<sub>13</sub> perovskite slab and a P3CT-BA like molecule containing a total of 862 atoms was simulated considering the same k-point grid and energy cutoff parameters than in the clean perovskite slab simulations.

The binding energy associated with the anchoring of P3CT-BA like molecules on the BA<sub>2</sub>MA<sub>3</sub>Pb<sub>4</sub>I<sub>13</sub> perovskite surface,  $E_{\text{bind}}$ , was calculated with the formula:

$$E_{\text{bin}} = E(\text{P3CT-BA@BA}_2\text{MA}_3\text{Pb}_4\text{I}_{13}) - E(\text{P3CT-BA}) - E(\text{BA}_2\text{MA}_3\text{Pb}_4\text{I}_{13}), \quad (1)$$

where the first term in the right-hand side of (1) represents the energy of the combined molecule-2D perovskite system, and the following two terms the energies of the integrating moieties. Likewise, the electronic charge density changes occurring in the BA<sub>2</sub>MA<sub>3</sub>Pb<sub>4</sub>I<sub>13</sub> perovskite surface upon P3CT-BA docking were estimated as:

$$\Delta\rho = \rho(\text{P3CT-BA@BA}_2\text{MA}_3\text{Pb}_4\text{I}_{13}) - \rho(\text{P3CT-BA}) - \rho(\text{BA}_2\text{MA}_3\text{Pb}_4\text{I}_{13}), \quad (2)$$

where  $\rho$  represents the electronic charge density of each indicated systems. Finally, the formation energy energy of BA and MA vacancies in the  $\text{BA}_2\text{MA}_3\text{Pb}_4\text{I}_{13}$  perovskite system,  $E_{\text{vac}}^{\text{BA}}$  and  $E_{\text{vac}}^{\text{MA}}$ , respectively, were computed through the expression:

$$E_{\text{vac}}^X = E_{\text{def}}(\text{BA}_2\text{MA}_3\text{Pb}_4\text{I}_{13}) + E(X) - E_{\text{perf}}(\text{BA}_2\text{MA}_3\text{Pb}_4\text{I}_{13}), \quad (3)$$

where  $E_{\text{def}}$  represents the energy of the system containing the molecular vacancy,  $E(X)$  then energy of an isolated BA or MA molecule, and  $E_{\text{perf}}$  the energy of the perfectly stoichiometric  $\text{BA}_2\text{MA}_3\text{Pb}_4\text{I}_{13}$  perovskite.

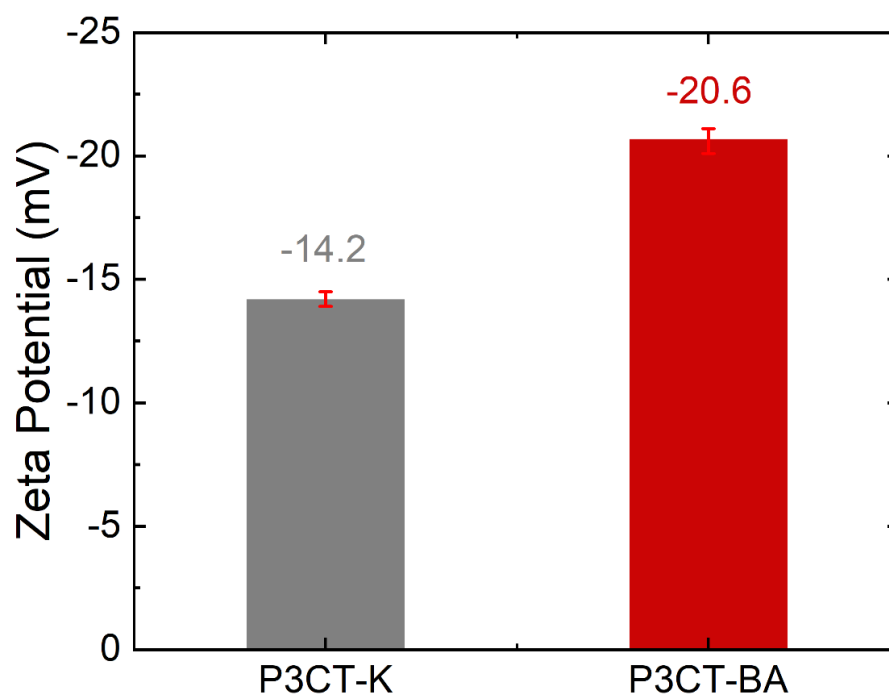


**Figure S1.** Zeta Potential of P3CT-K and P3CT-BA aqueous solutions.

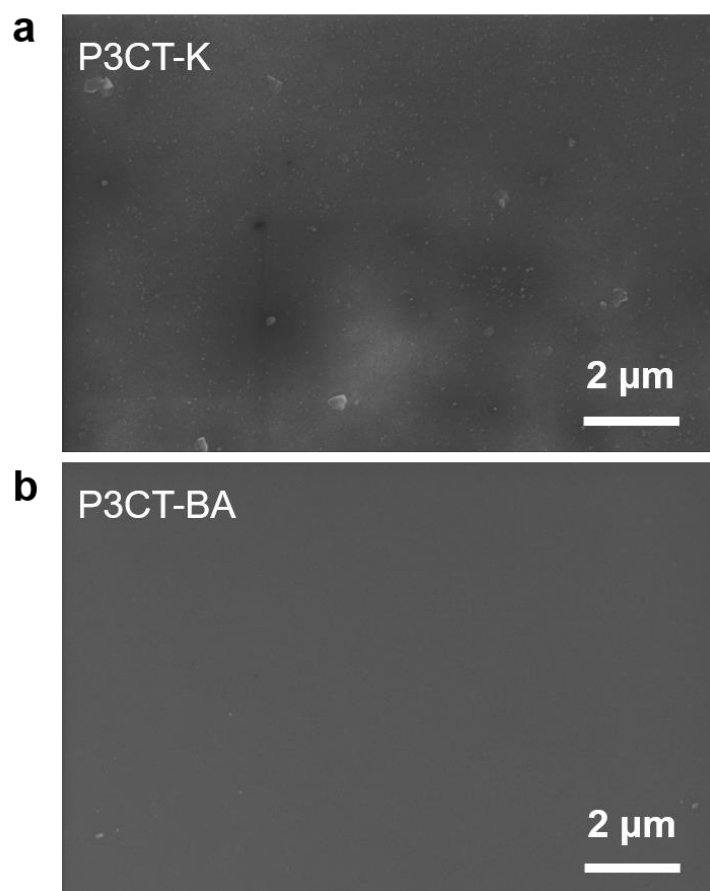


**Figure S2.** The SEM images of the P3CT-K (a) and P3CT-BA (b) films.

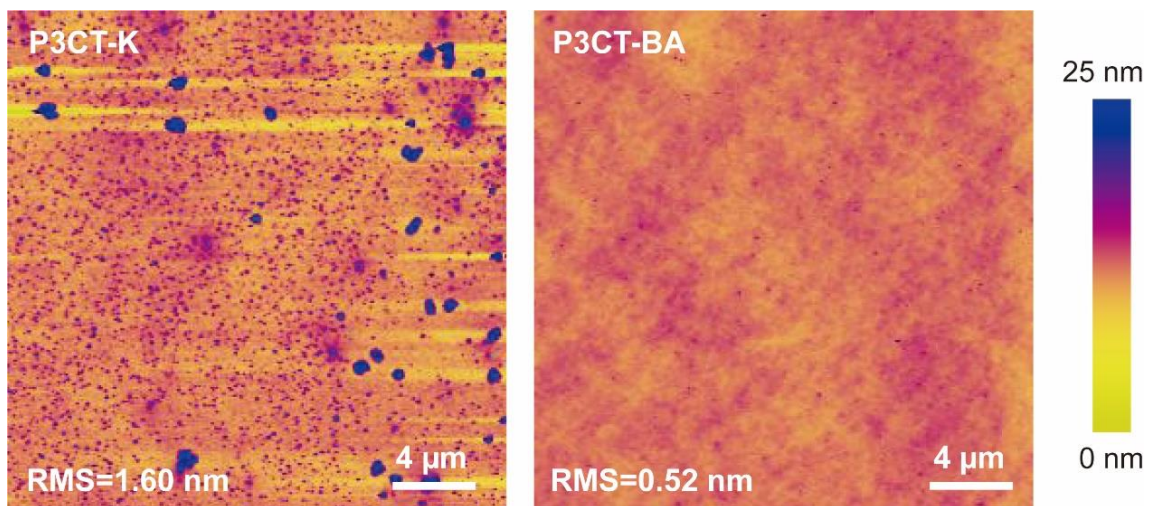


**Figure S3.** Height images of the large-sized P3CT-K (left) and P3CT-BA films (right).

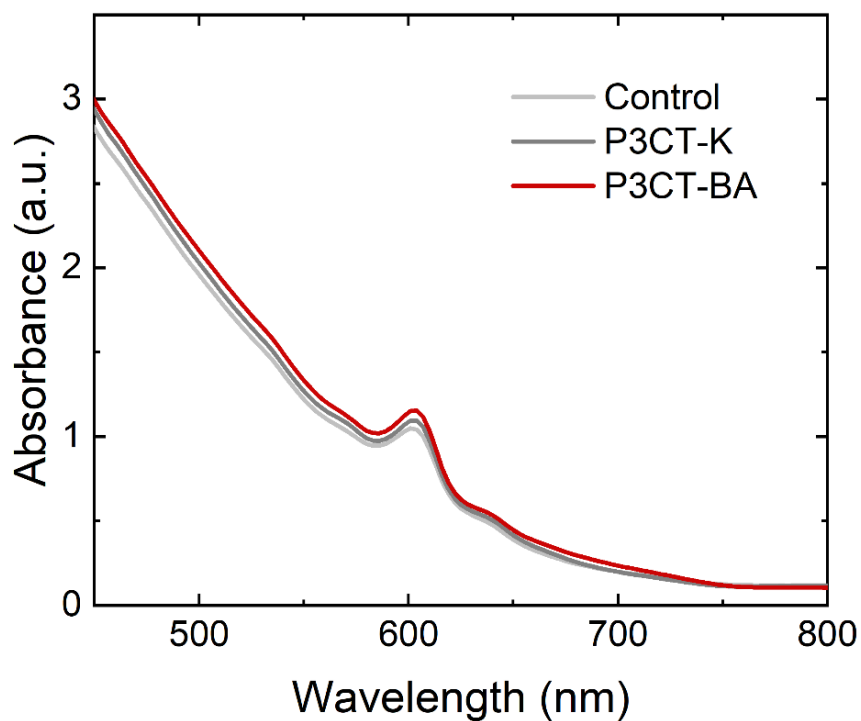


**Figure S4.** Absorption spectra of  $\text{BA}_2\text{MA}_3\text{Pb}_4\text{I}_{13}$  2D perovskite film deposited onto P3CT-K and P3CT-BA.

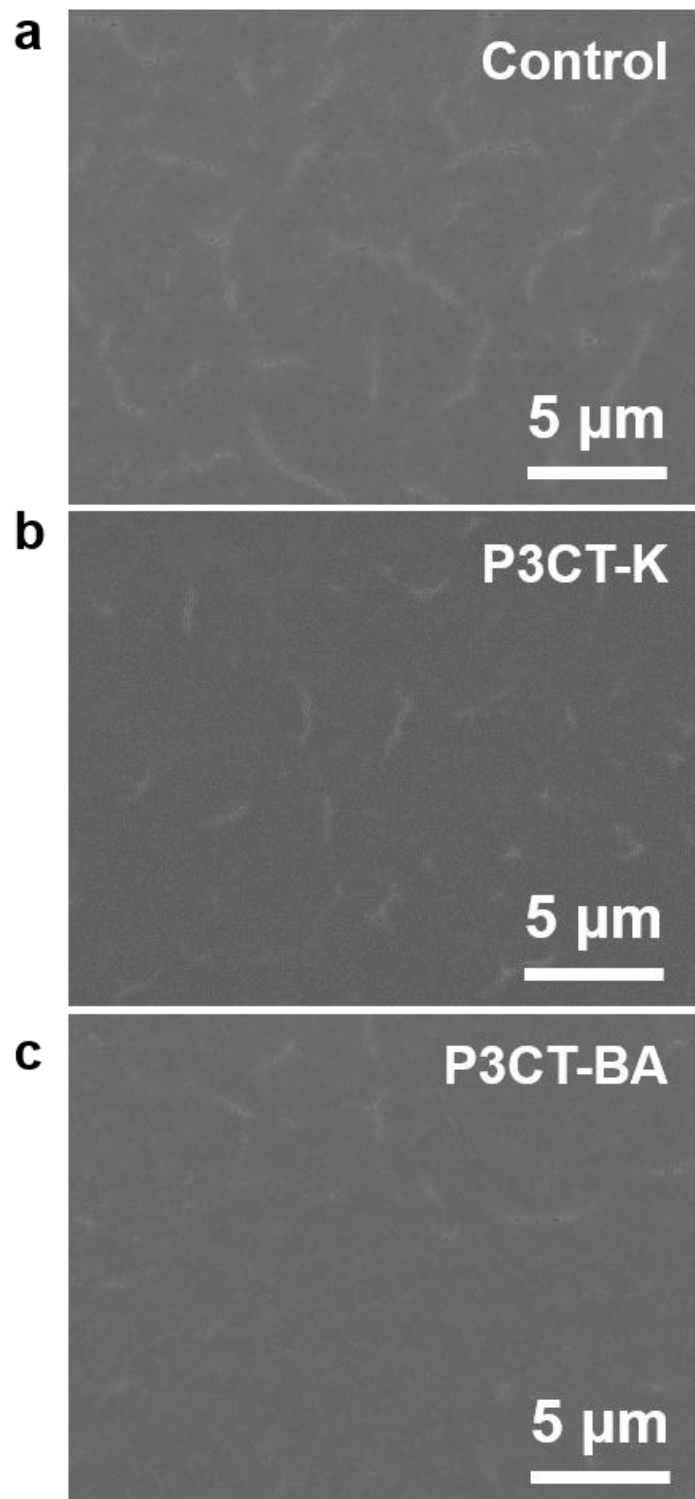


**Figure S5.** The SEM images of the  $\text{BA}_2\text{MA}_3\text{Pb}_4\text{I}_{13}$  2D perovskite films based on ITO (a), ITO/P3CT-K (b) and P3CT-BA (c) films.

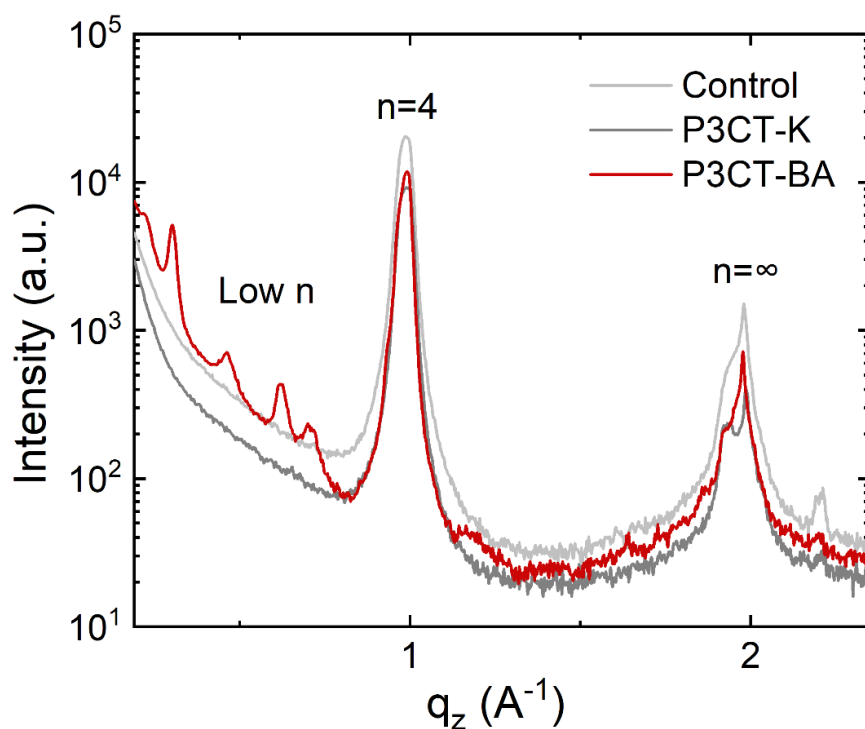


**Figure S6.** GIWAXS line-cut profiles (out-of-plane) of Quasi-2D perovskite films deposited on ITO, P3CT-K and P3CT-BA.

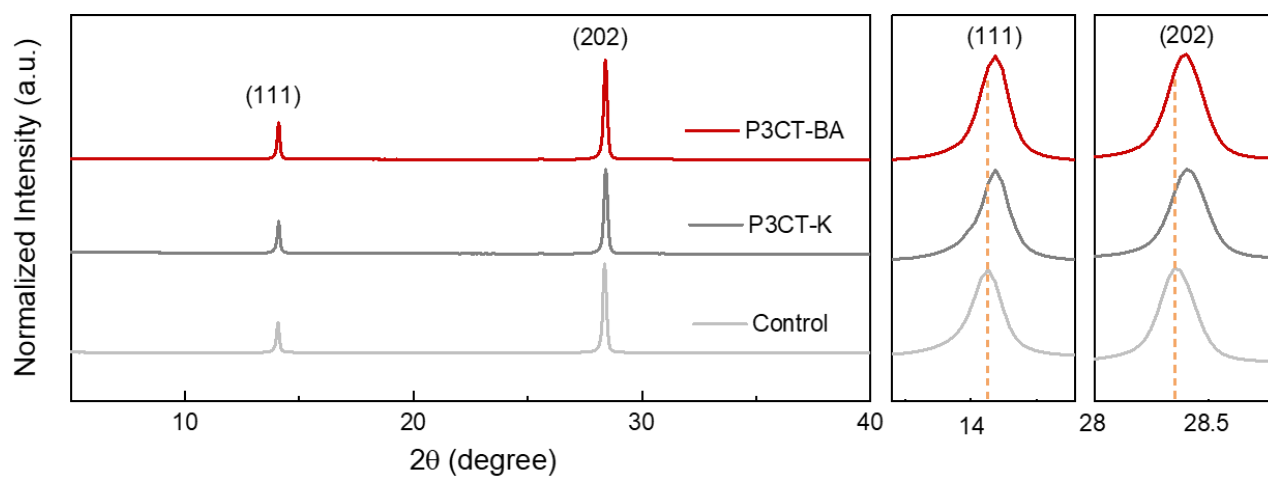


**Figure S7.** The XRD patterns of  $\text{BA}_2\text{MA}_3\text{Pb}_4\text{I}_{13}$  2D perovskite prepared on ITO, ITO/P3CT-K and ITO/P3CT-BA.

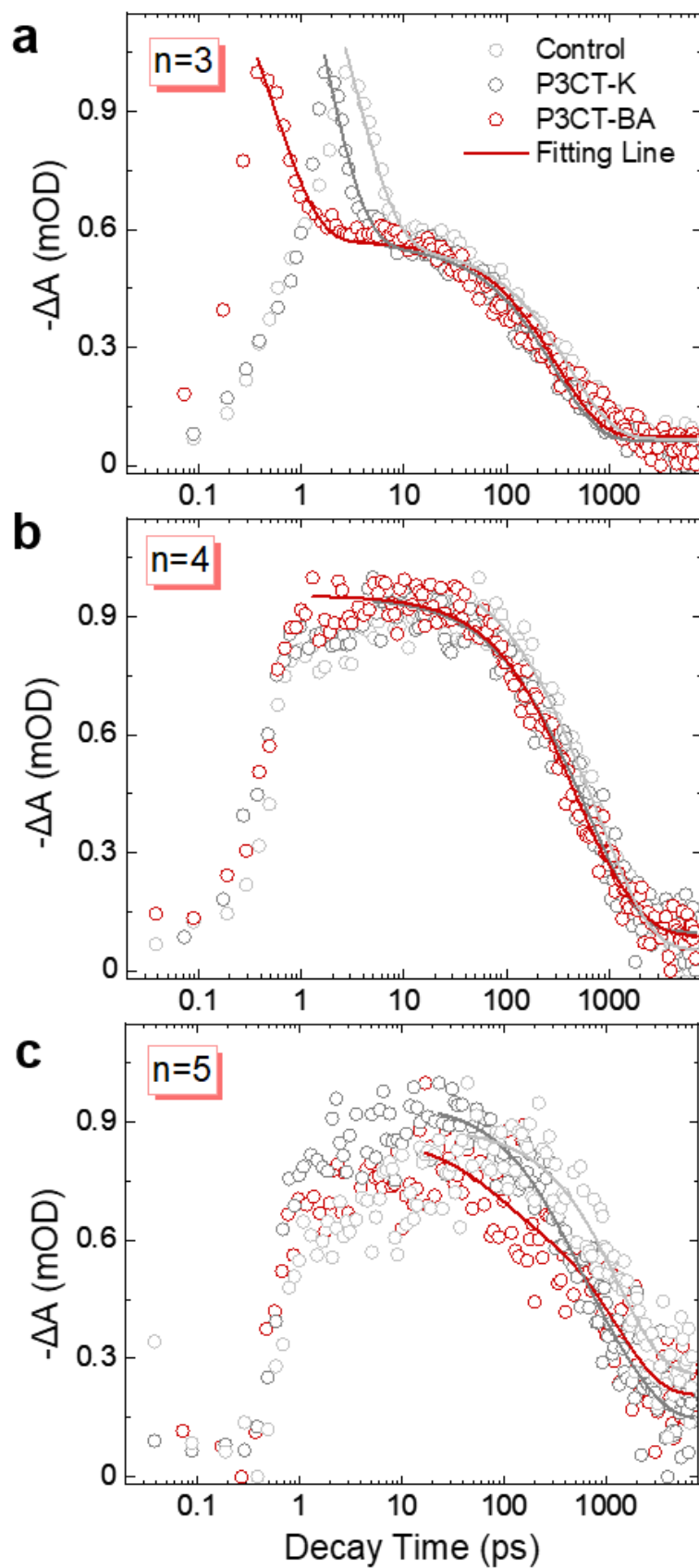


**Figure S8.** TA kinetics extracted from different GSB ( $n = 3, 4, 5$ ) for different films.

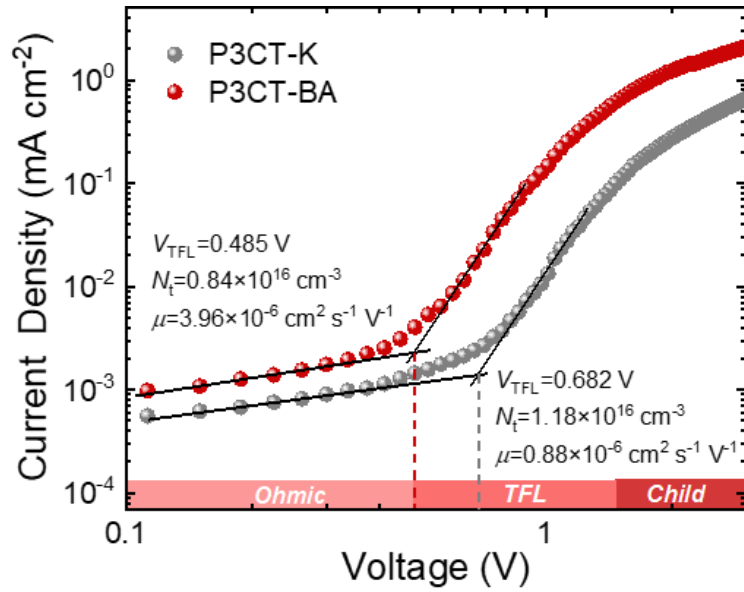


**Figure S9.** Dark current-voltage measurements of the hole-only devices for the control P3CT-K and P3CT-BA with a device structure of ITO/P3CT-X/Quasi-2D perovskite/Spiro-OMeTAD/Ag.

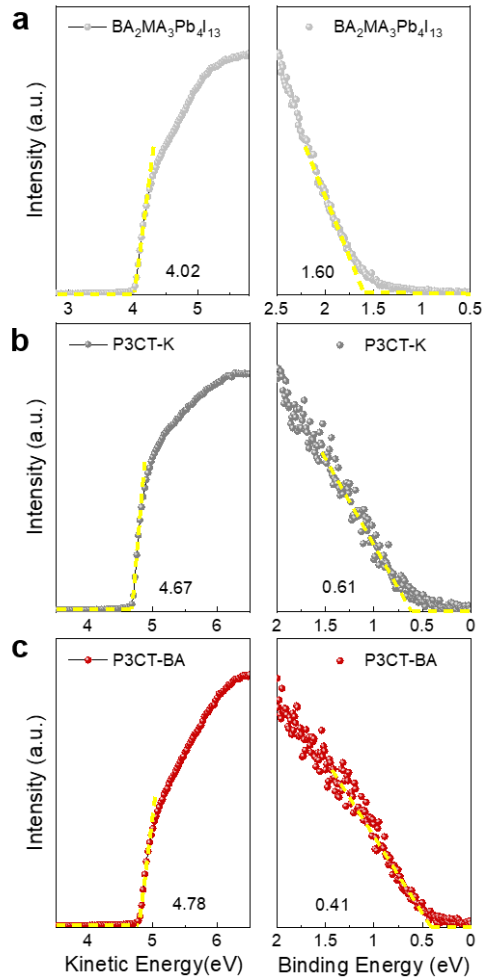


**Figure S10.** UPS spectra of BA<sub>2</sub>MA<sub>3</sub>Pb<sub>4</sub>I<sub>13</sub> 2D perovskite (a), P3CT-K (b) and P3CT-BA (c) film, the left panel of each shows the secondary electron cut-off region and the right one shows the magnified spectra near Fermi edge.

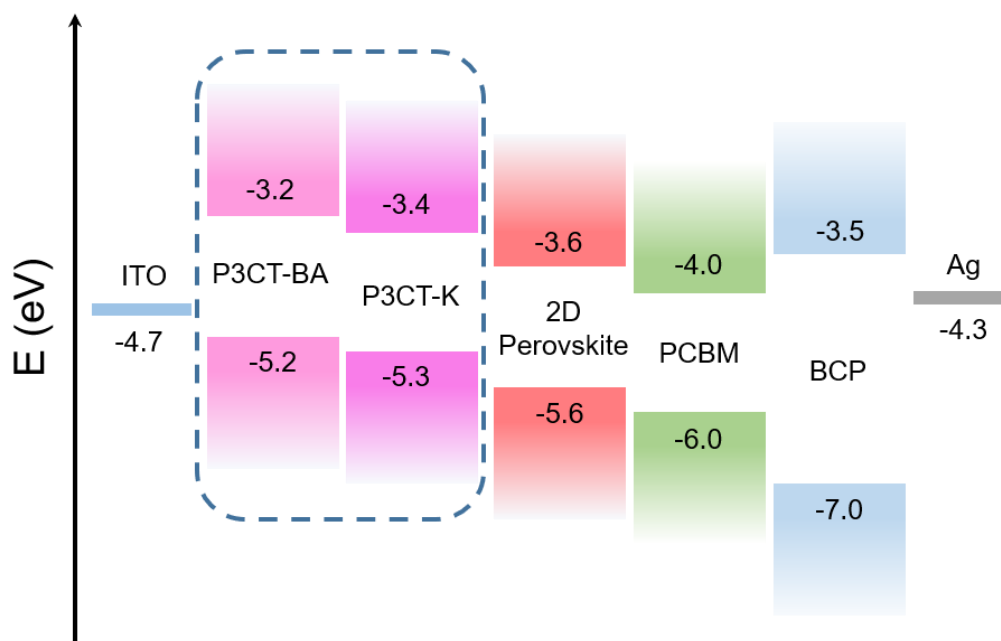


**Figure S11.** Band energy level diagram and corresponding bandgaps of the devices.

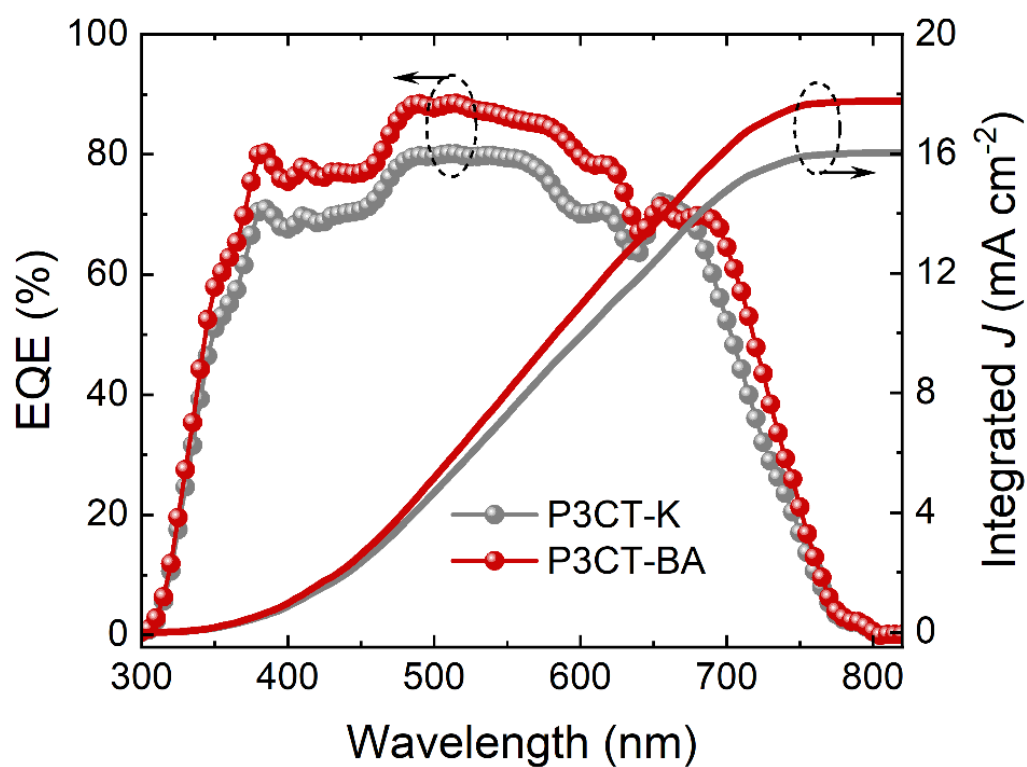


**Figure S12.** EQE spectra and integrated  $J_{sc}$  of the Quasi-2D devices based on P3CT-K and P3CT-BA.

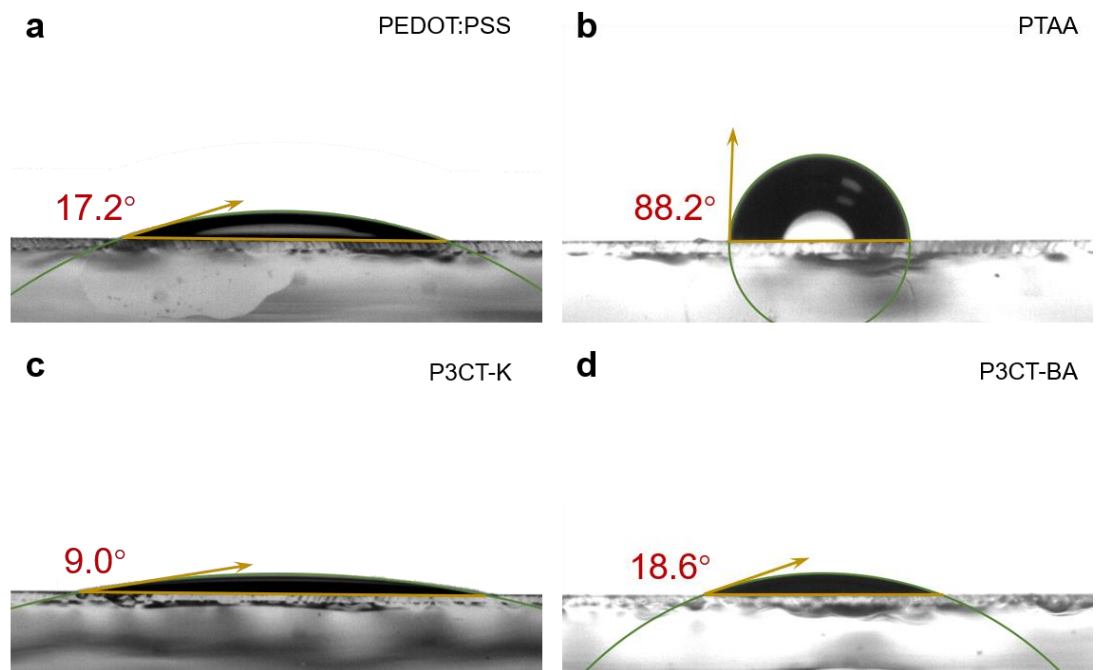


**Figure S13.** The contact angle of water on the PEDOT:PSS (a), PTAA (b), P3CT-K (c), P3CT-BA (d).

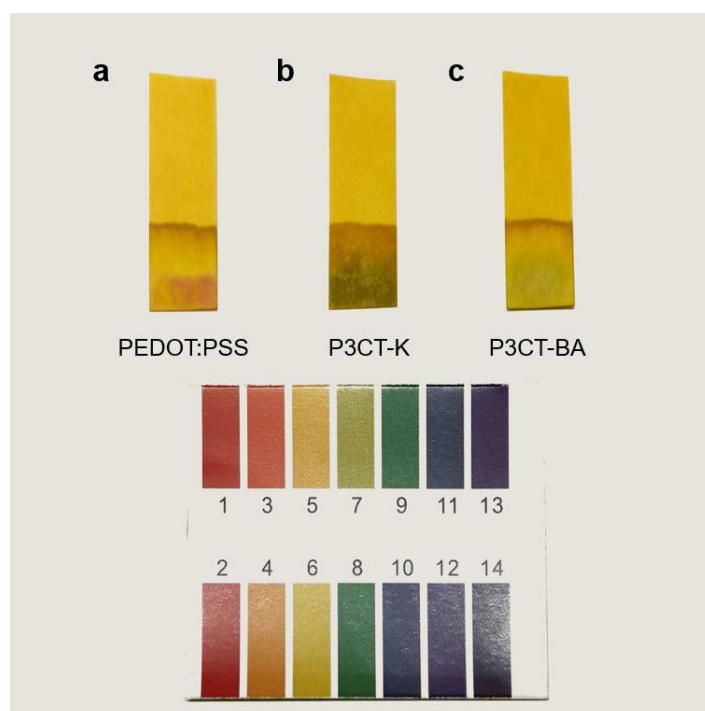


**Figure S14.** The pH value of PEDOT:PSS (a), P3CT-K (b), P3CT-BA (c) aqueous solution.

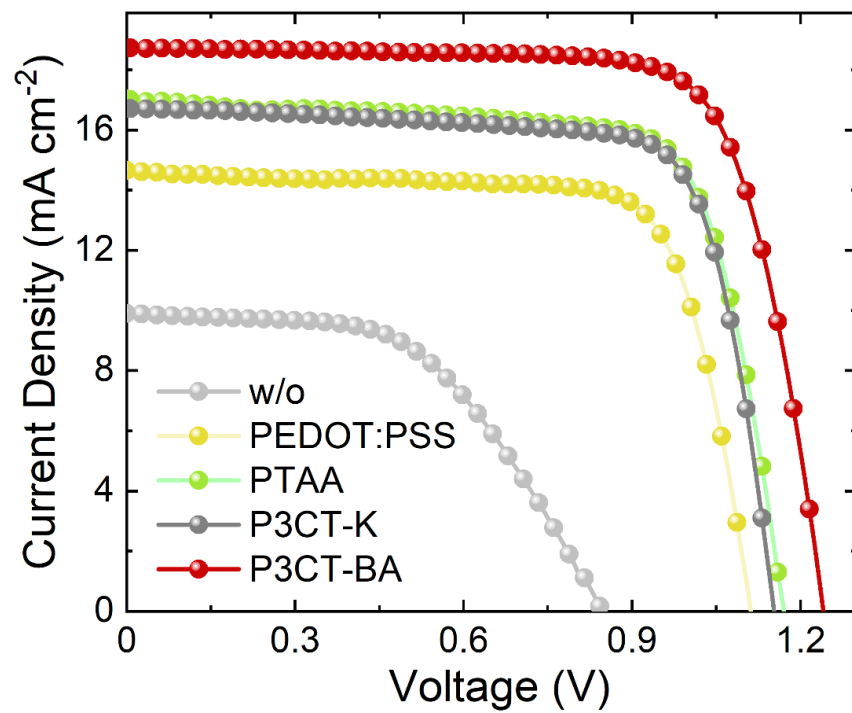


**Figure S15.**  $J$ - $V$  curves of the Quasi-2D devices based on different HTLs.

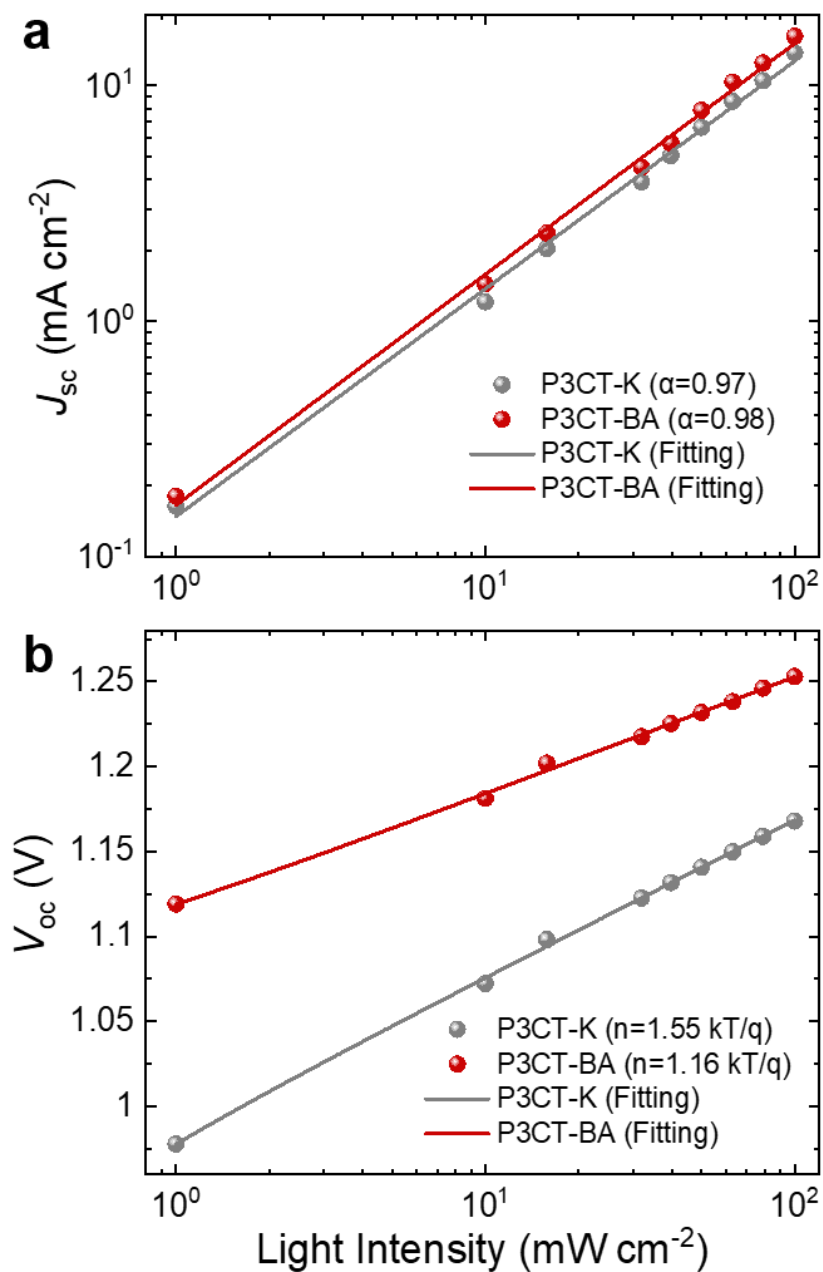


**Figure S16.**  $J_{sc}$  (a) and  $V_{oc}$  (b) as a function of light intensity of P3CT-K and P3CT-BA-based Quasi-2D devices.

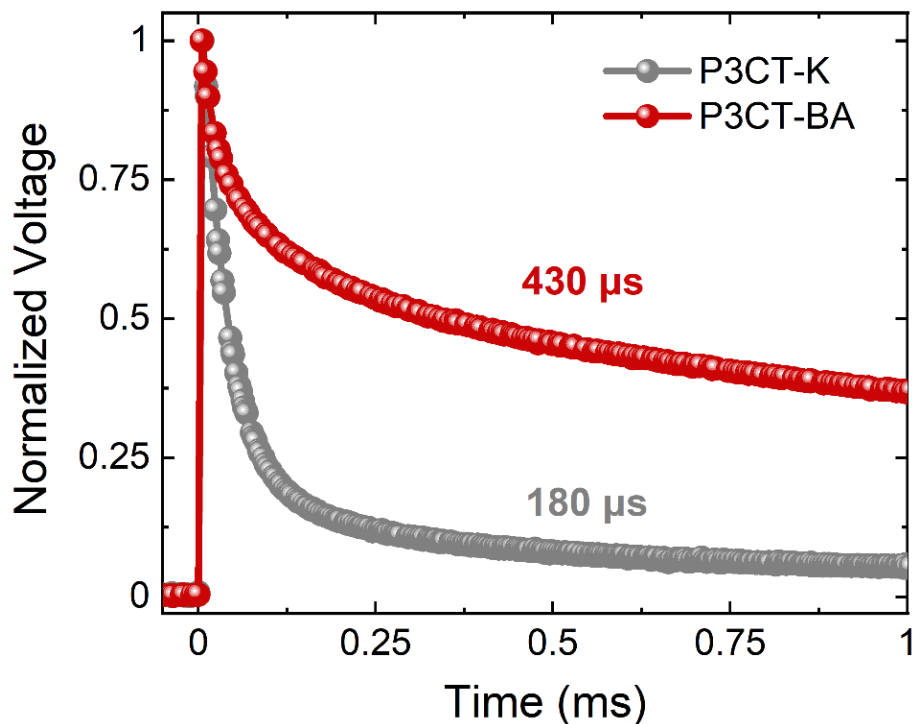


**Figure S17.** TPV measurements for Quasi-2D photovoltaics with P3CT-K and P3CT-BA.

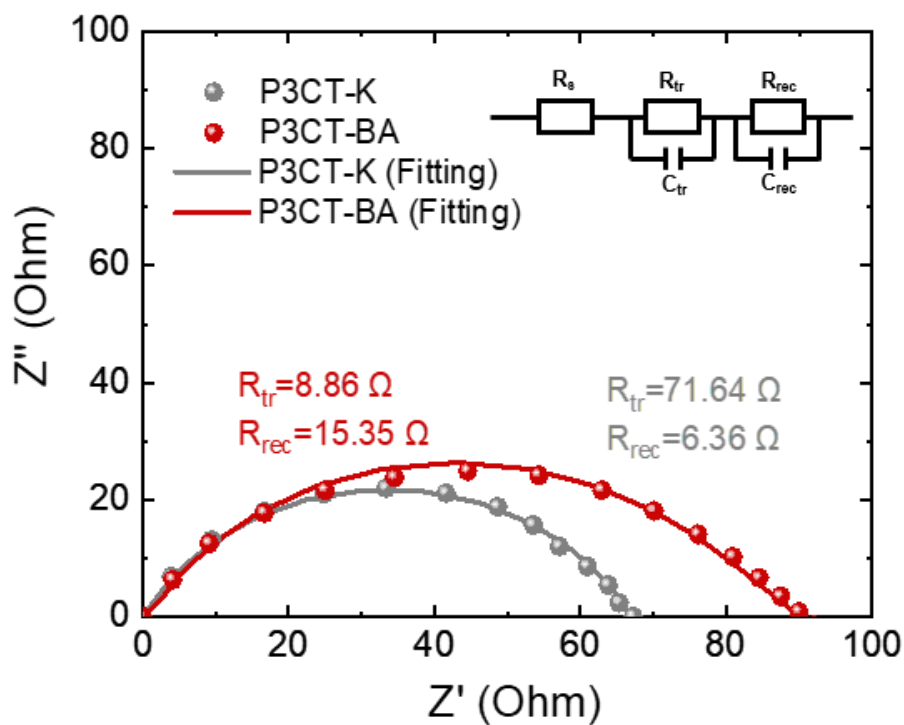


**Figure S18.** EIS measurements for Quasi-2D photovoltaics with P3CT-K and P3CT-BA.

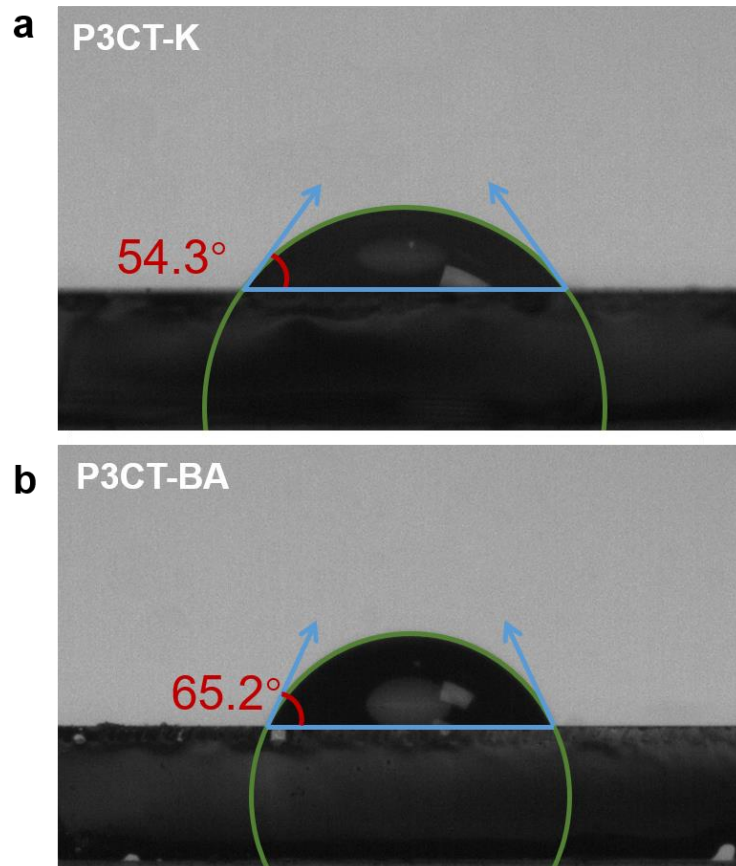


**Figure S19.** Snapshots of surface contact angle measurements for  $\text{BA}_2\text{MA}_3\text{Pb}_4\text{I}_{13}$  2D perovskite films with different HTLs based on water.

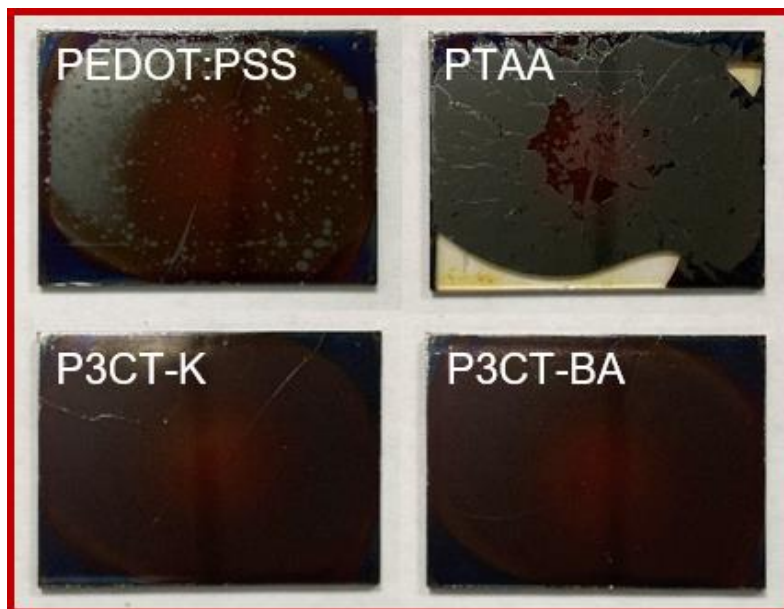


**Figure S20.** The surface condition of Quasi-2D perovskite films with PCBM/BCP based on different HTLs (PEDOT:PSS, PTAA, P3CT-K, P3CT-BA, respectively).

Table S1. Fitting parameters of decay amplitude and decay time obtained from TRPL spectra.

	$A_1$	$\tau_1$ (ns)	$A_2$	$\tau_2$ (ns)	$\tau_{avg}$ (ns)
Control	5198	0.71	297	16.28	9.55
P3CT-K	4389	0.74	366	12.85	7.91
P3CT-BA	5112	0.72	394	9.80	5.37

Table S2. Fitting parameters for the kinetics obtained from TA spectra,  $\tau_1$  and  $\tau_2$  are the fast decay and slow decay component.

		$A_1$	$\tau_1$ (ns)	$A_2$	$\tau_2$ (ns)	$\tau_{avg}$ (ns)
Control	n=3	1.17	3.20	0.49	414.50	407.05
	n=4	0.45	292.19	0.42	1073.93	953.94
	n=5	0.23	1320.11	0.40	1319.91	1319.98
P3CT-K	n=3	1.44	1.54	0.50	295.71	291.37
	n=4	0.23	208.96	0.74	1001.89	899.05
	n=5	0.35	337.22	0.45	1500.01	1327.52
P3CT-BA	n=3	0.92	0.54	0.49	209.67	208.67
	n=4	0.16	146.62	0.69	755.52	729.07
	n=5	0.17	72.46	0.48	1262.81	1238.72

Table S3. Optimization of the weight ratio of P3CT and BA (P3CT:BA).

Condition	$V_{oc}$ (V)	$J_{sc}$ (mA cm <sup>-2</sup> )	FF	PCE (%)
1:1.8	1.12	11.16	0.44	5.50
1:3.7	1.17	15.62	0.75	13.71
1:4.4	1.17	16.03	0.74	13.88
1:5.6	1.17	15.33	0.77	13.81

Table S4. Optimization of the concentration of P3CT-BA (mg/mL).

Condition	$V_{oc}$ (V)	$J_{sc}$ (mA cm <sup>-2</sup> )	FF	PCE (%)
0.5	1.15	13.32	0.70	10.85
1.0	1.16	13.61	0.77	12.15
1.5	1.18	16.32	0.78	15.02
2.0	1.19	17.01	0.78	15.81
2.5	1.18	16.78	0.75	14.85
3.0	1.16	15.85	0.72	13.24
4.0	1.16	15.02	0.73	12.72

Table S5. Optimization of the thickness of P3CT-BA.

Condition	Thickness (nm)	$V_{oc}$ (V)	$J_{sc}$ (mA cm <sup>-2</sup> )	FF	PCE (%)
2000 rpm	31	1.24	17.82	0.77	17.01
3000 rpm	20	1.25	18.67	0.76	17.74
4000 rpm	14	1.24	18.16	0.75	16.89
5000 rpm	12	1.24	17.64	0.76	16.63

Table S6. EIS parameters of devices based on P3CT-K and P3CT-BA.

	$R_s$ (Ohm)	$R_{tr}$ (Ohm)	$R_{rec}$ (Ohm)
P3CT-K	35.73	71.64	6.36
P3CT-BA	31.07	8.86	15.35

Table S7. Device parameters of minimodules based on P3CT-BA.

Number	$V_{oc}$ (mV)	$J_{sc}$ (mA cm <sup>-2</sup> )	FF	PCE (%)
1	6843.14	2.54	0.61	10.60
2	7055.39	2.53	0.58	10.35
3	7085.30	2.53	0.58	10.40
4	7127.19	2.52	0.58	10.42
5	7145.24	2.52	0.58	10.44
6	7586.85	2.52	0.53	10.13
7	7787.32	2.52	0.54	10.60
8	7864.31	2.51	0.55	10.86
9	7917.87	2.51	0.56	11.13

